

Observation of Magnetic-Field-Induced Laser Beam Deflection in Sodium Vapor

R. Holzner, P. Eschle, S. Dangel, R. Richard, H. Schmid, U. Rusch, and B. Röhricht
Physik-Institut der Universität Zürich, Winterthurerstrasse 190, CH-8057 Zürich, Switzerland

R. J. Ballagh, A. W. McCord, and W. J. Sandle
Physics Department, University of Otago, Dunedin, New Zealand
 (Received 14 November 1996)

A circularly polarized laser beam propagating through sodium vapor is shown to be deflected by the inhomogeneous magnetic field from a nearby electric current-carrying thin wire aligned parallel to the beam. The effect arises from the refractive index gradient induced by magnetic-field-modified optical pumping. The experimentally observed beam deflection is in good agreement with predictions from a $J = 1/2 \leftrightarrow J = 1/2$ model for the full four-dimensional spatialtemporal evolution of the interaction between radiation field and atoms. The time of order 100 ns needed for the beam to switch between undeflected and deflected positions is determined by the average Larmor precession period and is 2 orders of magnitude shorter than the optical pumping time. [S0031-9007(97)03129-3]

PACS numbers: 42.25.Bs, 32.80.Bx, 42.25.Ja, 42.62.Hk

The interaction between light and matter provides one of the most enduring interests in physics. A main aspect of this field—the mechanical motion of atoms induced by light—includes topics ranging from the contemporary one of laser cooling to the classical problem of radiation pressure in stars. The conjugate subject—the manipulation of light by matter—is an even broader scientific and technical field. Emphasis in the latter area has mostly been on light-atom coupling through the electric dipole interaction which is many orders of magnitude larger than the magnetic-dipole interaction. However, magnetic effects, though small in absolute terms and not previously emphasized, may dominate behavior in an appropriately chosen system. Laser beam deflection in an atomic vapor placed in a *homogeneous* magnetic field is in principle possible, and has indeed been observed [1] with a circularly polarized laser beam in a 50 G transverse magnetic field. However, the presence of some additional spatial symmetry-breaking interaction is required to provide a significant deflection [2]. In Ref. [1], a glass interface is employed to introduce magnetic circular dichroism of Cs atoms. This leads to a deflection of about $1.5 \mu\text{rad}$. We present here a simple arrangement in which symmetry breaking is intrinsic to the experiment, arising from a magnetic-field *gradient*. Specifically, we demonstrate control of laser beam propagation by a spatially inhomogeneous magnetic field for a circularly polarized laser beam traveling through sodium vapor parallel to a current-carrying wire. Deflection of the beam is 3 orders of magnitude larger than reported in [1], and is essentially due to the transverse magnetic-dipole density gradient established by a local competition between optical-pumping-induced creation and magnetic-field-induced destruction of the orientation of atomic magnetic dipoles. Related effects which also involve substantial, but purely light-induced beam deflections are the spatial separation of circularly polarized laser beams in an atomic vapor [3] and the mutual deflec-

tion of left- and right-hand circularly polarized laser beams [4] by establishing adjacent regions of opposite atomic magnetic-dipole orientations. With regard to possible applications these effects provide “control of light by light” while the experimental evidence of “magnetic control of light deflection” presented in this Letter may be of relevance for novel electrically driven devices to be used in optical communication or optical computing systems. The observed deflection which is sufficient to switch a laser beam between, e.g., two optical fibers, occurs for a relatively low electric current, low atomic density, and, therefore, low laser beam intensity. As numerical simulations indicate, the deflection could be increased by about a factor of 2 for experimentally less favorable but still realistic values of atomic density, beam power, beam waist, detuning, electrical current, or the distance between the laser beam and the electrical current-carrying wire.

In the experiment (see Fig. 1) a dye-laser beam propagates with its axis $90 \mu\text{m}$ from a $20 \mu\text{m}$ diameter wire

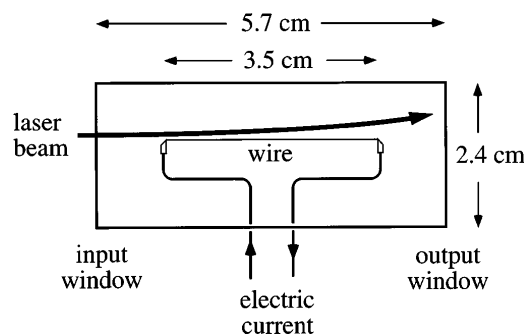


FIG. 1. Cylindrical Pyrex-glass cell with current-carrying wire. Residual magnetic fields are compensated to within about 3 mG of zero by three orthogonal pairs of Helmholtz coils. The gold-plated $20 \mu\text{m}$ diameter tungsten wire is clamped by copper fittings right at the top of the 1 mm thick tungsten holding wires sealed into the cell.

passing through a glass cell containing sodium vapor and argon buffergas at 205 °C. The beam waist of 50 μm is adjusted to be at the beginning of the wire to within ± 0.2 cm. The role of the argon, at a pressure of 230 mbar, is to suppress the effects of hyperfine structure while permitting optical pumping in the effective $J = 1/2$ ground state. The diffusion rate of sodium atoms is drastically reduced: this inhibits nonlocal effects, increases the transient time of sodium in the laser beam, and leads to a low value for the magnetic-dipole dephasing rate ($\Gamma_l = 4.7 \times 10^4 \text{ s}^{-1}$) essential for efficient optical pumping in the relatively low power beam (6 mW at the entry point to the vapor). A further consequence of the buffer gas in collisionally broadening the transition (optical dipole dephasing rate $\Gamma_{lu} = 1.0 \times 10^{10} \text{ s}^{-1}$ is large compared to the natural radiative decay rate of the excited state $\gamma = 6.25 \times 10^7 \text{ s}^{-1}$) is that dispersive and absorptive effects are comparable at the experimental laser detuning (1.7 GHz above the peak absorption frequency of the homogeneously broadened D_1 transition). The difference between undeflected and deflected beam positions at the cell output window is recorded by a CCD camera with a pixel resolution of 5 μm . In order to suppress background noise effects the position of the beam is determined by spatial averaging over all pixels brighter than 50% of maximum. An important issue with the setup is that the electric current of 60 mA needed to produce an appreciable steady-state beam deflection—28 μm measured at the cell output window as shown in Fig. 2 (top)—gives rise to a slight temperature change in the wire. After about 5 ms the heating effect causes the local sodium density to rise and leads to an increase of beam deflection. “Steady-state” deflections [Fig. 2 (bottom)] are recorded between 1–30 μs after current initiation, sufficiently delayed to avoid the initial transients in beam displacement but before the onset of thermal effects. These measurements were carried out using a stroboscopic recording technique as described in [3].

The basic mechanism can be understood by considering the effect in terms of an encoding/diffraction sequence [5]. A somewhat oversimplified view (which ignores the spatial variation of intensity across the beam as well as absorptive effects) is that the optically pumped medium can be approximated as a glass prism of refractive index less than unity. The “thick” edge of the prism is adjacent to the wire where the high magnetic field inhibits optical pumping, and the medium has a near-normal (linear value of) refractive index. Further from the wire, where the magnetic field is insufficiently large to suppress optical pumping, the medium is bleached with a refractive index tending towards free space; here, the prism has its “thin” edge. The net effect of the prism is to phase encode the laser beam and bend the propagation direction away from the wire.

This picture can be developed semiquantitatively in analytical terms. The behavior of the medium is best under-

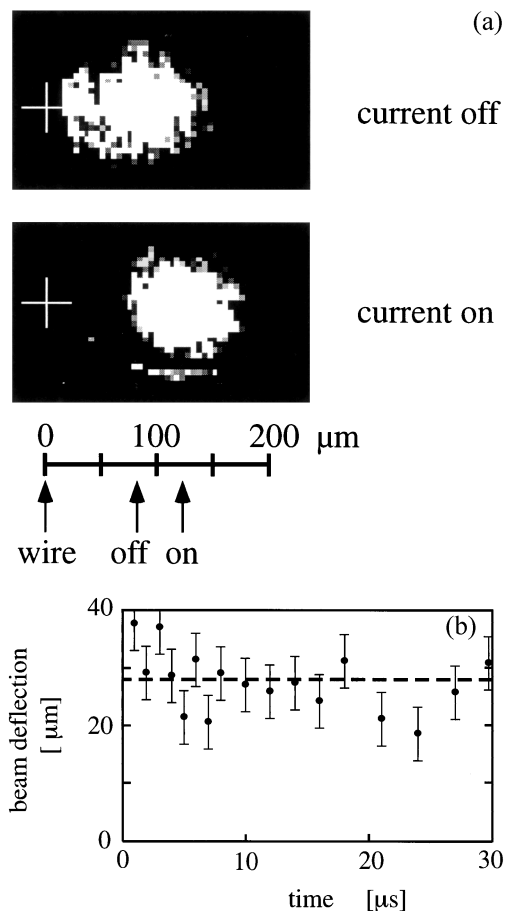


FIG. 2. Top: Undeflected and deflected beam spots at the output window of the sodium vapor cell before and after the electric current through the wire has been switched on. For the determination of the beam positions only pixels brighter than 50% of maximum are considered. Bottom: Beam deflection during the first 30 μs after the current has been switched on. Error bars indicate the standard deviation of ten measurements taken within 3 min. The main causes for the scatter of single measurements are the fluctuation of the input laser intensity as well as density fluctuations inside the vapor cell. The dashed line marks the mean deflection of $(28 \pm 2) \mu\text{m}$ averaged over the displayed series of 17 times ten measurements.

stood in terms of a response function η_+ which is defined in Eq. (5) of Ref. [6], and related to the refractive index n of the medium by $n = 1 - (\alpha_0 c / 2\omega) \text{Im}[\eta_+]$, where α_0 is the weak-field resonant absorption coefficient. The additional phase that is imparted on the field by the medium after a propagation distance z_{enc} is $\phi_{\text{enc}} = -\alpha_0 z_{\text{enc}} \text{Im}[\eta_+] / 2$. An explicit form for η_+ is given by employing a $J = 1/2 \leftrightarrow J = 1/2$ transition to model the D_1 line [7]:

$$\eta_+ = \frac{(1 + i\Delta)}{1 + \Delta^2 + (2\beta' + 4)I}. \quad (1)$$

Here, $I = |\mathcal{E}_+ / E_{\text{sat}}|^2$ is the intensity (with \mathcal{E}_+ the positive frequency σ^+ -polarized component of the electric field propagating initially along the z direction, and E_{sat}

a saturation field defined in Ref. [6]), Δ is the laser-atom detuning in units of the optical dipole dephasing rate, and β' is a function describing the effect of optical pumping, discussed further below. The response function is essentially zero in the center of the beam where the intensity is large, but in the beam edges where the intensity falls below the critical value $I_{\text{crit}} = (1 + \Delta^2)/(2\beta' + 4)$, the dispersive response $\text{Im}[\eta_+]$ is approximately $\Delta/(1 + \Delta^2)$.

The effect of the magnetic field is expressed by the parameter β' . In general β' is a complicated expression, but in the regime of interest in this Letter, where the radiative decay rate $\gamma \gg \Gamma_l$, it can be written as $\beta' \approx \gamma/\Gamma'_l$, where Γ'_l is an effective lower-level orientation decay rate. Γ'_l increases rapidly with the ground-state Larmor frequency ω_B [see [7] and Eq. (2) of Ref. [8]] and for large magnetic fields I_{crit} takes the value

$$I_{\text{crit}} \approx \frac{(1 + \Delta^2)}{4}; \quad \text{for } \omega_B > \gamma\sqrt{(1 + \Delta^2)}, \quad (2)$$

while for small magnetic fields it takes the much smaller value

$$I_{\text{crit}} \approx (1 + \Delta^2)\frac{\Gamma_l}{2\gamma}; \quad \text{for } \omega_B < \sqrt{\gamma\Gamma_l(1 + \Delta^2)}. \quad (3)$$

These equations reflect the fact that for a pure σ^+ field, saturation occurs by optical pumping of the atoms into the $m = +1/2$ ground state. A transverse magnetic field causes Larmor precession of the ground-state magnetic dipoles about the magnetic field, and, consequently, as the magnetic field increases, the laser intensity I_{crit} needed to achieve optical pumping increases. For a Gaussian beam, the critical intensity occurs at a transverse distance $d_c = w_0\sqrt{(\ln I_{00})}/2$ from the beam center, where w_0 is the beam waist and $I_{00} = (2\beta' + 4)I_{00}/(1 + \Delta^2)$ (and where I_{00} is the on-axis intensity). The distance d_c is smaller on the side of the beam closest to the wire.

An upper limit of the bending angle of the beam is estimated by assuming phase encoding to be significant only on the high-magnetic-field edge of the beam nearest the wire. In the subsequent diffractive propagation, the center of the beam occurs where the *optical* paths from each edge of the beam are equal, and so the geometric difference in the paths must compensate for the phase encoding of ϕ_{enc} . This leads to the estimate for the maximum bending angle of $\theta_{\text{max}} \approx \phi_{\text{enc}}\lambda/4\pi d_c$, and using an encoding distance [5] $z_{\text{enc}} = [8z_R(1 + \Delta^2)/\alpha_0|\Delta|\ln I_{00}]^{1/2}$, where z_R is the free space Rayleigh length, we finally obtain

$$\theta_{\text{max}} \approx \frac{w_0\sqrt{\alpha_0|\Delta|}}{2\ln(I_{00})\sqrt{z_R(1 + \Delta^2)}}. \quad (4)$$

The validity of this expression is restricted to the dispersive regime [5], and for simple tractability we evaluate I_{00} in the large magnetic-field regime ($\beta' \rightarrow 0$). This leads under the conditions of the experiment to an upper estimate for the deflection angle of 1.8 mrad which, con-

sidering the approximations involved, is in reasonable agreement with the experimental value of ≈ 0.6 mrad.

To confirm the validity of this physical picture we have modeled the experiment using the spatially and temporally dependent Maxwell-Bloch equation

$$\left[\left(\frac{\partial}{\partial z} + \frac{1}{c} \frac{\partial}{\partial t} \right) - \frac{ic}{2\omega} \left(\frac{\partial^2}{\partial x^2} + \frac{\partial^2}{\partial y^2} \right) \right] \mathcal{E}_+(\mathbf{r}, t) = \frac{i\omega}{2c\epsilon_0} \mathcal{P}_+(\mathbf{r}, t). \quad (5)$$

The macroscopic polarization (\mathcal{P}_+) is self-consistently determined by the solution of Eq. (5) in conjunction with the time-dependent atomic density matrix equations for homogeneously broadened $J = 1/2 \leftrightarrow J = 1/2$ atoms [see Eq. (3) of Ref. [6]]. The density-matrix equations have the same form as those given in Ref. [9], but with additional terms describing the effects of the transverse magnetic field. These computationally intensive equations have been solved on a NEC SX-3/24R supercomputer. In Fig. 3 we present simulation results showing how the spatial distribution of the field intensity evolves.

When there is no electric current, the beam establishes an undeflected steady-state profile after about 20 μs [Fig. 3(a)]. Upon application of the current at $t = 0$ the beam quickly deflects to its final position: Fig. 3(b) gives the situation after 50 ns. The reason for this rapid response is that the magnetic field depolarizes the ground state within a fraction of an average Larmor period (i.e., submicrosecond); on the other hand, decay of the transients as shown in Fig. 2 (bottom) will take several average Larmor periods and arises through the magnetic-field inhomogeneity as well as atom diffusion. Although the deflection suffers little further change the output intensity at beam center continues to grow as optical pumping becomes more complete, and eventually a steady state is achieved, as shown in Fig. 3(c), 20 μs after the current is turned on. The simulated beam deflection in the final steady state, 34 μm , is in good agreement with experiments shown in Fig. 2, given that all parameters used in the theory correspond to experimentally determined values without fitting. The destruction rate Γ_l of the ground-state orientation includes the effects of radiation trapping [10,11] and is determined as described in [12]. The inverse of Γ_l determines the upper limit to the time scale for reaching equilibrium intensity. We have also used the simulations to test the accuracy of Eq. (4). Over a wide range of parameters Eq. (4) consistently overestimates the bending angle by a factor of approximately 3. The principal reason for the overestimation is our simplifying assumption that the magnetic field is “large” throughout the half of the beam closest to the wire, and is “small” in the other half.

In summary, we have demonstrated that a laser beam propagating through an atomic vapor may be magnetically controlled in direction, and that the magnitude of

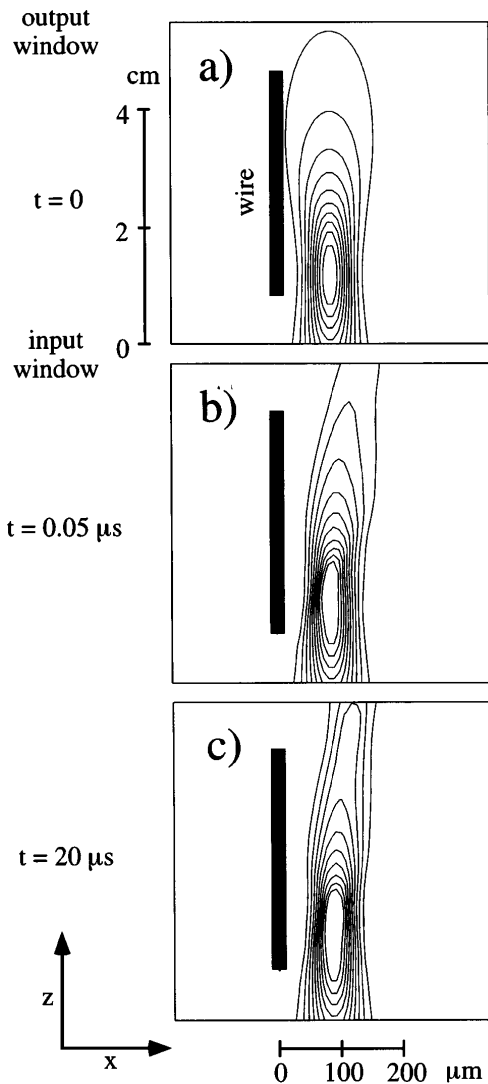


FIG. 3. Intensity contour plots of the laser beam in the $y = 0$ plane from the simulation: (a) steady state with no current; (b) 50 ns after the current is turned on; (c) steady state 20 μs after current is turned on. The wire is parallel to the z axis at $x = 90 \mu\text{m}$, $y = 0$. From 6 mW input-beam power, 5.5 mW penetrates the vapor in (a) and 1.8 mW in (c).

deflection arising from an electric current in an adjacent thin wire is in good accord with a simple phase-encoding/diffraction picture. An important issue is that the steady-state density distribution of absorbing atoms can change much faster by the application of a transverse mag-

netic field gradient than by optical pumping. The four-dimensional spatial-temporal $J = 1/2 \leftrightarrow J = 1/2$ model we present describes the steady-state behavior accurately: with respect to the fast time scale on which the deflection is established, the diffusion of atoms in and out of the beam is of minor importance. The model, however, cannot describe slower dynamic effects associated with Larmor oscillation damping, optical pumping, or the diffusion of atoms in the true dynamical time scale [13,14]. Preliminary results from a more general model including hyperfine structure are in excellent agreement with the time-resolved experimental observations and confirm the validity of the $J = 1/2 \leftrightarrow J = 1/2$ picture for calculations of the steady-state deflection.

We thank K. Bösiger and D. Schnarwiler for the most skillful fabrication of the sodium vapor cell as well as the Swiss Scientific Computing Center for access to their supercomputing facilities. This work was supported by the Schweizer Nationalfonds and the Ernst Hadorn Stiftung.

- [1] R. Schlessler and A. Weis, *Opt. Lett.* **17**, 1015 (1992).
- [2] Angular momentum conservation of circularly polarized light interacting with sodium atoms can lead to a very small beam displacement (in the order of 20 nm) as shown in T. Blasberg and D. Suter, *Phys. Rev. Lett.* **69**, 2507 (1992).
- [3] B. Röhrlich *et al.*, *J. Opt. Soc. Am. B* **12**, 1411 (1995).
- [4] R. Holzner, P. Eschle, A. W. McCord, and D. M. Warrington, *Phys. Rev. Lett.* **69**, 2192 (1992).
- [5] A. McCord, R. Ballagh, and J. Cooper, *J. Soc. Am. B* **5**, 1323 (1988).
- [6] A. W. McCord and R. J. Ballagh, *J. Opt. Soc. Am. B* **7**, 73 (1990).
- [7] D. McClelland, Ph.D. thesis, University of Otago, Dunedin, New Zealand, 1988.
- [8] A. Wilson *et al.*, *Opt. Commun.* **110**, 365 (1994).
- [9] R. Ballagh and N. Mulgam, *Phys. Rev. A* **52**, 4945 (1995).
- [10] M. Schiffer, G. Ankerhold, E. Cruse, and W. Lange, *Phys. Rev. A* **49**, R1558 (1994).
- [11] D. Tupa and L. W. Anderson, *Phys. Rev. A* **36**, 2142 (1987).
- [12] B. Röhrlich *et al.*, *Phys. Rev. A* **50**, 2434 (1994).
- [13] S. Dangel *et al.*, *J. Opt. Soc. Am. B* **12**, 681 (1995).
- [14] D. Suter and J. Mlynek, *Adv. Magn. Opt. Res.* **16**, 1 (1992).